Made available courtesy of National Academy of Sciences: http://www.nationalacademies.org/

Functional coding variation in recombinant inbred mouse lines reveals multiple serotonin transporter-associated phenotypes

Ana M. D. Carneiro[a], David C. Airey[a], Brent Thompson[a], Chong-Bin Zhu[a], Lu Lu[b,c], Elissa J. Chesler[d], Keith M. Erikson[e], and Randy D. Blakely[a,f,g,1]

[a]Departments of Pharmacology, [f]Psychiatry, and [g]Center for Molecular Neuroscience, Vanderbilt University School of Medicine, Nashville, TN 37232-8548; [b]Key Laboratory of Nerve Regeneration, Nantong University, Nantong 226001, China; [c]Department of Anatomy and Neurobiology, University of Tennessee Health Science Center, Memphis, TN 38163; [d]BioSciences Division, Oak Ridge National Laboratory, Oak Ridge, TN 37831-6420; and [e]Department of Nutrition, University of North Carolina, Greensboro, NC 27402-6170

Edited by Floyd E. Bloom, The Scripps Research Institute, La Jolla, CA, and approved December 5, 2008 (received for review September 24, 2008)

The human serotonin (5-hydroxytryptamine, 5-HT) transporter (hSERT, *SLC6A4*) figures prominently in the etiology and treatment of many prevalent neurobehavioral disorders including anxiety, alcoholism, depression, autism, and obsessive-compulsive disorder (OCD). Here, we use naturally occurring polymorphisms in recombinant inbred (RI) lines to identify multiple phenotypes associated with altered SERT function. The widely used mouse strain C57BL/6J, harbors a SERT haplotype defined by 2 nonsynonymous coding variants [Gly-39 and Lys-152 (GK)]. At these positions, many other mouse lines, including DBA/2J, encode, respectively, Glu-39 and Arg-152 (ER haplotype), amino acids found also in hSERT. Ex vivo synaptosomal 5-HT transport studies revealed reduced uptake associated with the GK variant, a finding confirmed by in vitro heterologous expression studies. Experimental and in silico approaches using RI lines (C57BL/6J × DBA/2J = BXD) identify multiple anatomical, biochemical, and behavioral phenotypes specifically impacted by GK/ER variation. Among our findings are several traits associated with alcohol consumption and multiple traits associated with dopamine signaling. Further bioinformatic analysis of BXD phenotypes, combined with biochemical evaluation of SERT knockout mice, nominates SERT-dependent 5-HT signaling as a major determinant of midbrain iron homeostasis that, in turn, dictates iron-regulated DA phenotypes. Our studies provide an example of the power of coordinated in vitro, in vivo, and in silico approaches using mouse RI lines to elucidate and quantify the system-level impact of gene variation.

gene | haplotype | iron | serotonin | dopamine

A complex set of phylogentically conserved traits relies upon the production, secretion, and inactivation of the biogenic amine 5-HT (1). A critical and conserved mechanism to regulate 5-HT signaling involves the action of the presynaptic 5-HT transporter, SERT (2). SERTs are not only responsible for the clearance of 5-HT after release, but also recycle synaptic 5-HT to sustain adequate stores for 5-HT release (3).

The recognition of the central role played by SERT in 5-HT inactivation has been reinforced by studies where mouse SERT (mSERT) has been eliminated (4), suppressed (5, 6), or enhanced (7). Although investigations with these models provide critical support for a role of SERT in presynaptic 5-HT clearance and homeostasis, inferences linking SERT to neural signaling and behavior are complicated by significant compensatory changes in other genes (8). Conversely, a lack of recognition for background genetic diversity in mouse strains likely limits the full elaboration of phenotypes associated with SERT genetic variation (9). Indeed, SERT knockout mice display different phenotypes depending on their genetic background (10).

An alternative approach is the identification of traits that are sensitive to naturally occurring polymorphisms using genetic reference populations, such as BXD recombinant inbred (RI) lines (11). BXD RI lines are isogenic, homozygous mosaics of C57BL/6J and DBA/2J inbred strains, previously created by inbreeding F_2 intercross progeny. Conventionally, these populations are used in forward genetic screens to discover unknown polymorphisms affecting a trait. Here we analyze RI lines that share specific 5-HT gene variants against an otherwise randomized genetic background, an advantage over approaches that test allele effects on one or two inbred backgrounds (11–13). Perhaps the greatest strength of this approach is the availability of archived, dimensional data across a large number of phenotypes linked to individual BXD lines (14, 15), including anatomical, neurochemical, and behavioral traits. In this report, we initiate investigation of naturally occurring variation in 5-HT genes via analysis of functional coding polymorphism in mSERT. Furthermore, as this archive is a freely accessible, expanding resource, appreciation for how SERT and 5-HT-linked gene variants impact physiology can be increasingly enriched as additional phenotypes are registered. This integrative approach to reverse genetics of identified polymorphisms should also be applicable to more powerful genetic reference populations (13, 16, 17).

Our report initiates with an analysis of the distribution among laboratory mouse strains, followed by neurochemical analyses of SERT function in synaptosomes from several standard inbred lines. Subsequently, we confirm reduced 5-HT transport mSERT phenotype associated with the GK variant in a heterologous expression system. Controlling for *Tph2* variation, we replicate haplotype effects in vivo using select BXD lines then exploit the BXD population to expand analyses to anatomical, biochemical, and behavioral phenotypes. Through this approach, we document multiple SERT-sensitive phenotypes and elucidate a connection to iron homeostasis that we propose links 5-HT signaling to dopamine (DA) modulated behaviors.

Results

Identification of Slc6a4 Coding Variation in Inbred Mouse Lines. Analysis of *Slc6a4* DNA sequences from 40 mouse inbred lines deposited in the Mouse Phenome database (http://aretha.jax.

Author contributions: A.M.C., D.C.A., K.M.E., and R.D.B. designed research; A.M.C., B.T., C.-B.Z., and K.M.E. performed research; L.L. and E.J.C. contributed new reagents/analytic tools; A.M.C., D.C.A., B.T., C.-B.Z., and K.M.E. analyzed data; and A.M.C., D.C.A., B.T., C.-B.Z., L.L., E.J.C., K.M.E., and R.D.B. wrote the paper.

The authors declare no conflict of interest.

This article is a PNAS Direct Submission.

Freely available online through the PNAS open access option.

[1]To whom correspondence should be addressed. Medical Research Building III, Rm 7140, Vanderbilt School of Medicine, Nashville, TN 37232-8548. E-mail: randy.blakely@vanderbilt.edu.

This article contains supporting information online at www.pnas.org/cgi/content/full/0809449106/DCSupplemental.

© 2009 by The National Academy of Sciences of the USA

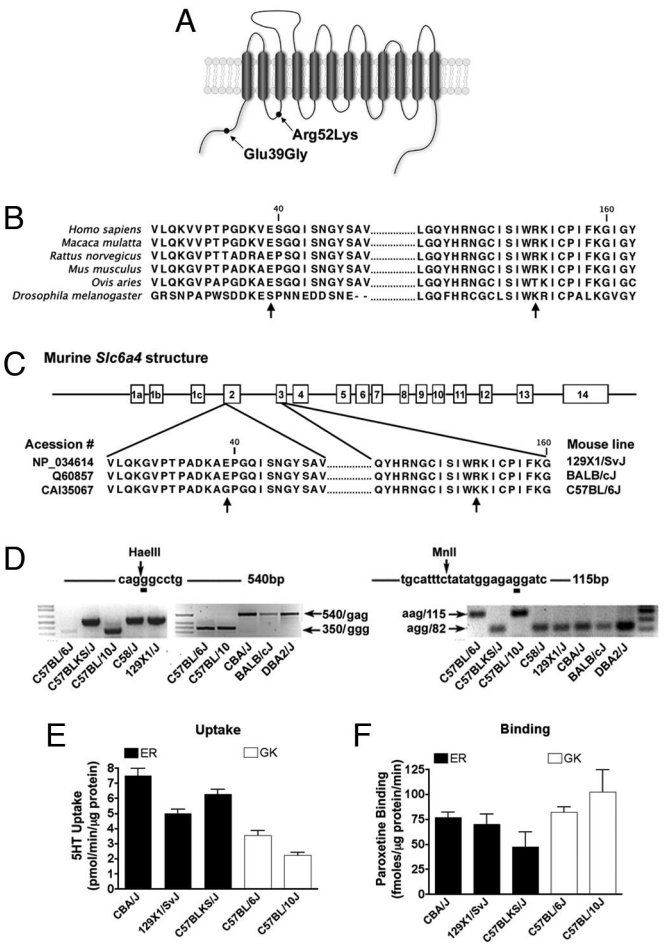

Fig. 1. Identification of a naturally occurring *Slc6a4* haplotype in inbred mouse lines. (*A*) Schematic illustration of the location of the *Slc6a4* SNPs characterized in this study. (*B*) Alignment of SERT protein sequences from human, macaque, rat, mouse, sheep, and fruit fly. (*C*) Alignment of National Center for Biotechnology Information mSERT protein sequences with Glu39Gly and Arg152Lys polymorphisms indicated by arrows. (*D*) Genotyping by PCR-RLFP of C57BL/6J, C57BLKS/J, C57BL/10J, C58/J, 129 × 1/SvJ, CBA/J, BALB/cJ, and DBA/2J mice. Digestion of a 540-bp band by HaeIII with a generation of a 350-bp band indicates G (Gly) allele in the Glu39Gly SNP. The 213-bp amplicon generated by PCR was subjected to restriction digestion with MnlI to detect the G SNP (Arg) resulting in a digestion product of 82 for the R allele or 115 for the K allele. (*E*) Midbrain 5-HT synaptosomal uptake in ER (CBA/J, 129/SvJ, and C57BLKS/J) and GK (C56BL/6J and C57BL/10J) lines. (*F*) Midbrain [^{3}H]paroxetine binding in ER (CBA/J, 129/SvJ, and C57BLKS/J) and GK (C56BL/6J and C57BL/10J) lines.

org/pub-cgi/phenome/mpdcgi?rtn = docs/home) revealed a haplotype consisting of 2 nonsynonymous SNPs (Fig. 1*A* and *C*) that distinguish C57BL/6J, C57BL/10J, C57BL/10ScSr, C57BR/cdJ, C57L/J, PERC/EiJ, and RBA/DnJ strains from other mouse lines. We confirmed mSERT variation using a PCR-RFLP-based strategy (see Fig. 1*D* and Table S1) and by direct sequencing of *Slc6a4* in selected lines. The first transition (rs13481111) converts the highly conserved amino acid Glu-39 (gag) within the mSERT cytosolic NH2 terminus to Gly (ggg) (Fig. 1 *A* and *C*). The second transition (rs29413009) converts an Arg codon (agg) to one encoding Lys (aag) at amino acid 152 in the transporter's first intracellular loop (Fig. 1 *A* and *C*). These 2 variants constitute a distinct haplotype (hereafter denoted as mSERT ER or GK) as they have not segregated in the establishment of inbred mouse lines, consistent with their separation by only 2,476 bp of genomic sequence.

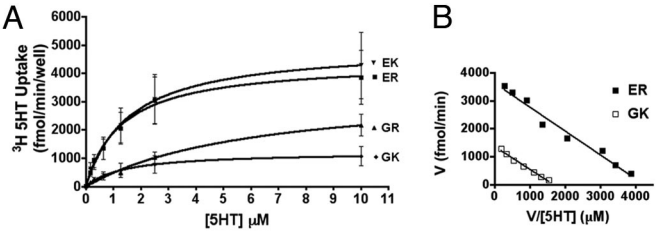

Fig. 2. Functional characterization of mSERT coding variation in HEK-293 cells. (*A*) Saturation kinetic studies show a reduced 5-HT uptake in cells transfected with the 39G single mutation (▲) and 39G and 152K double mutation (GK, □) when compared with the 39E, 152R isoform found in most inbred mouse lines (ER, ■). (*B*) Scatchard plot of ER and GK data generated from saturation uptake analysis. Data presented as means ± SEM from 6 independent experiments.

Characterization of the Slc6a4 Haplotype in Inbred Mouse Lines. For initial inspection of functional differences between *mSERT* ER and GK, we compared 5-HT uptake rates in midbrain synaptosomes prepared from multiple strains discordant for the 2 haplotypes, but concordant for the same, high functioning *Tph2* genotype, a potentially confounding factor (18) (Table S1). Strains bearing the GK haplotype (C57BL/6J and C57BL/10J) demonstrated significantly reduced 5-HT uptake as compared with strains carrying the ER haplotype (CBA/J, 129/SvJ, and C57BLKS/J) (Fig. 1*E*, nested ANOVA, $F(1, 3) = 12.21$, $P = 0.039$, $\eta^2 = 0.61$). These functional differences could not be attributed to changes in mSERT density, as levels of [^{3}H]paroxetine binding did not differ across strains (Fig. 1*f*, nested ANOVA, $F(1, 3) = 6.34$, $P = 0.086$). Haplotype-associated differences in midbrain mSERT activity could not be ascribed to general alterations in ion gradients or membrane potential because no differences were observed in dopamine or norepinephrine transport across the same preparations (Fig. S1*A*). Consistent with the identity of the *Tph2* isoforms across these lines, we also found no differences in midbrain or cortical 5-HT or 5-HIAA tissue levels that might account indirectly for uptake differences (Fig. S1*B*).

Characterization of Coding Variants in mSERT-Transfected HEK-293 Cells. Unknown genetic variation that cosegregates with ER/GK could underlie the differences in 5-HT uptake in synaptosomes. We therefore monitored mSERT activity in HEK-293 cells transfected with full-length transporter cDNAs. Here again, kinetic analyses revealed significantly lower SERT activity associated with the GK haplotype (Fig. 2*A*, 2-way ANOVA, $P < 0.0001$, $n = 6$, $\eta^2 = 0.17$), with changes arising from a significant, 4-fold reduction in 5-HT transport V_{MAX} (Fig. 2*B*; ER, 4414 ± 715 fmol/min, $n = 6$; GK, 1219 ± 274 fmol/min $n = 6$, unpaired Student's *t test*, $P < 0.01$, Cohen's $d = 2.77$) but no discernible haplotype impact on 5-HT transport K_M (ER, 2.970 ± 0.808; GK, 1.041 ± 0.056). As with inbred line studies, no overall differences in total mSERT expression were observed either by Western blots or by membrane binding assays using the cocaine analog [^{125}I]RTI-55 (data not shown). These measures yield an estimate of SERT catalytic rate of GK SERT ~50% that of ER SERT. Analysis of cDNAs expressing individual variants indicates that the reduced SERT activity of the GK haplotype arises from the Glu-39 substitution (Fig. 2*A*, 2-way ANOVA, $P < 0.0001$, $n = 6$, $\eta^2 = 0.15$, Bonferroni's post hoc test, $P < 0.05$).

Impact of Slc6a4 Variation in Recombinant Inbred Mouse Lines Concordant for the Pro-447 Tph2 Allele. To establish a systems-level evaluation of 5-HT genetic variation, we extended our investigation of mSERT GK/ER-associated phenotypes to (BXD) lines. By determining the status of RI strains for *Slc6a4* and *Tph2*

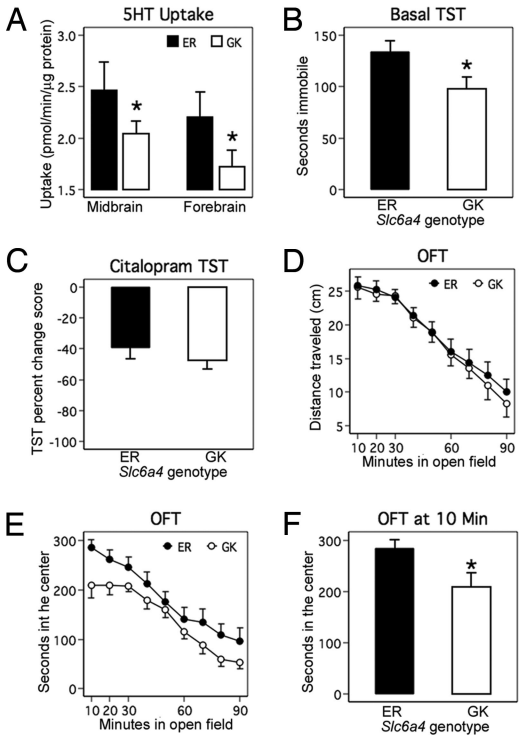

Fig. 3. Characterization of mSERT ER/GK haplotypes in recombinant inbred BXD lines. (*A*) Reduced midbrain and forebrain 5-HT uptake in GK RI mouse lines compared with EK RI mouse lines. (*B*) Reduced basal immobility time in GK RI mouse lines compared with ER RI mouse lines. (*C*) ER and GK mouse lines have similar sensitivity to the SSRI citalopram (20 mg/kg) as assessed by TST (EK, $n = 88$ mice; GK, $n = 71$ mice). (*D*) Basal locomotor behavior is not altered in GK lines. (*E*) GK RI lines spend less time in the center of the open field apparatus than ER lines over a 90-min period. (*F*) Novel open field test for exploratory activity shows reduced time in the center for mice bearing the GK *Slc6a4* .

variants, we were able to identify and acquire 27 BXD strains concordant for the common, high-functioning C57BL/6J *Tph2* allele (Pro-447) that could be divided into 13 lines with the *Slc6a4* DBA/2J ER haplotype (nos. 9, 11, 31, 39, 40, 45, 50, 56, 63, 66, 75, 76, 83) and 14 lines with the *Slc6a4* C57BL/6J GK haplotype (nos. 43, 44, 48, 51, 60, 61, 67, 69, 73, 77, 90, 92, 96, 97). We prepared midbrain and forebrain synaptosomes from 7 lines of each *Slc6a4* haplotype and determined SERT activity. BXD RI lines bearing the GK haplotype demonstrated reduced 5-HT uptake in midbrain and forebrain synaptosomes (mixed model, likelihood ratio test (LRT) of genotype effect across brain areas, χ^2 (df = 1) = 3.95, $P = 0.047$, $\eta^2 = 0.25$) (Fig. 3*A*). As expected, 5-HT uptake was significantly higher in midbrain than in forebrain (LRT χ^2 (df = 1) = 6.65, $P = 0.010$, $\eta^2 = 0.07$) and genotype was equally penetrant in both brain regions (i.e., interaction was not significant, LRT χ^2 (df = 1) = 0.01, $P = 0.932$) (Fig. 3*A*). These findings reinforce our conclusion that the *Slc6a4* GK haplotype exhibits reduced 5-HT transport activity.

We assessed BXD lines bearing GK and ER for differences in levels of 5-HT and metabolites. Although again no significant differences were found (data not shown), tissue measurements of neurotransmitters are a fairly insensitive indication of synaptic 5-HT availability and action. We therefore sought a behavioral readout known to be sensitive to SERT function (19, 20). We tested BXD lines in marble burying, nestlet shredding, basal tail suspension, and open field tests, each known to be sensitive to selective serotonin reuptake inhibitor (SSRI) drugs or SERT ablation (10, 20, 21). Although no significant differences between ER and GK lines were detected in either marble burying or nestlet shredding behaviors (Fig. S2), lines expressing the reduced function GK variant exhibited significantly decreased basal tail suspension immobility (Fig. 3*b*, unpaired Student's *t test*, $P = 0.037$, Cohen's $d = 0.88$). Immobility in the tail suspension test (TST) is believed to reflect diminished capacity for stress-alleviating behaviors, and reduced SERT function achieved with acute SSRI treatment decreases immobility (22). Despite differences in basal TST immobility, sensitivity to citalopram (20 mg/kg) appeared identical between genotypes (shown as % reduction in immobility over saline, Fig. 3*C*). When we tested GK and ER lines for their locomotor response to an open field, we found horizontal activity to be indistinguishable (Fig. 3*D*), suggesting a lack of impact of mSERT variants on overall motor function or psychomotor activation. Nonetheless, GK lines differed from ER lines in time spent in the chamber center, often considered a measure of anxiety (Fig. 3 *E* and *F*, unpaired Student's *t test*, $P = 0.020$, Cohen's $d = 0.79$).

In Silico Identification of Phenotypes Influenced by Slc6a4 Coding Variation. To identify unique phenotypes affected by ER/GK variation, we performed an in silico analysis of 843 archived BXD phenotypes registered at Genenetwork.org (11) including anatomical, biochemical, and behavioral traits. We analyzed trait dependence on genotype using a 2-gene model comprising independent effects of the *Slc6a4* ER/GK and *Tph2* Arg447Pro variants and allowing for gene–gene interaction. Fig. S3 shows phenotypes more associated with the independent effects of the mSERT GK haplotype, and include several traits linked to alcohol sensitivity or tolerance, including mean and total ethanol consumption and ethanol-conditioned taste aversion, consistent with previous findings in SERT knockout mice (23, 24). Traits influenced by interactions of *Slc6a4* and *Tph2* variants are provided in Table S2 (independent *Tph2*-associated traits are presented in Table S3).

An assessment of archived biochemical traits revealed the GK haplotype to be associated with ventral midbrain dopamine D2 receptor (*Drd2*) expression, and caudate-putamen dopamine transporter (*Slc6a3*) density (Fig. 4 *A* and *B*). Interestingly, a prior analysis has revealed that these (and other) DA-related phenotypes are associated with midbrain iron levels (25). Consistent with these findings, the GK mSERT haplotype associates significantly with elevated iron levels in both the region of DA cell bodies (ventral midbrain) and DA terminal fields (caudate-putamen) (Fig. 4 *C* and *D*).

To test whether the changes observed in iron levels are the result of genetic variation in SERT vs. that of a gene in linkage disequilibrium, we measured brain iron levels in *Slc6a4*$^{-/-}$ (KO) mice. SERT KO mice exhibit significantly reduced midbrain iron levels (Fig. 4*D*, −/−: 4.123 ± 0.5349 $n = 11$; +/+: 6.678 ± 0.3762 $n = 8$, unpaired *t test* $P < 0.005$, Cohen's $d = 1.53$). Hippocampal tissue did not differ in iron levels (−/−: 8.973 ± 1.327 $n = 12$; +/+: 8.466 ± 1.644 $n = 10$, unpaired *t test*, $P = 0.810$).

Discussion

In this study, we characterize a naturally occurring haplotype in the mSERT gene, where Gly-39 and Lys-152 replace Glu-39 and Arg-152, respectively. Our findings are of general relevance in that they illustrate an integrative approach to identifying quantitative phenotypes influenced by mouse genetic variation. More specifically, our findings capitalize on naturally occurring variation in mSERT to establish a platform for associating molecular and system level phenotypes of 5-HT signaling genes.

RI lines with the mSERT GK haplotype displayed reduced basal immobility in the TST, consistent with ex vivo and transfected cell studies that identify reduced SERT activity with the GK variant. Nonetheless, the reduced SERT activity in the GK lines is still adequate for acute potentiation of 5-HT signaling by

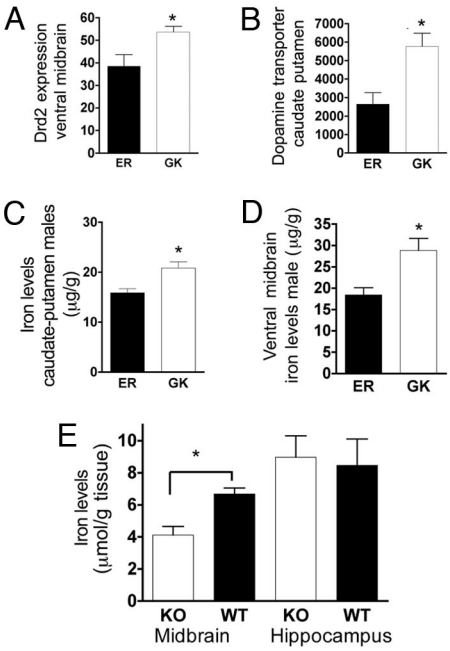

Fig. 4. DA phenotypes and brain iron levels are influenced by SERT gene variation. (*A* and *B*) DA-signaling phenotypes: D2 receptor expression in ventral midbrain (10591541) and DAT expression in caudate-putamen (10591541). (*C* and *D*) GK (□) lines have increased ventral midbrain iron levels in both caudate-putamen and midbrain when compared with ER (■) lines. (*E*) *Slc6a4*$^{-/-}$ mice (□) have reduced midbrain iron levels when compared with wild-type controls (■). Unpaired Student's *t* test *P* values are indicated above bars.

an SSRI (citalopram). One might expect that reduced SERT activity might have resulted in altered citalopram responsiveness; however, the dosage of citalopram optimized for responses in the TST paradigm may simply be above that required to distinguish SSRI sensitivities in vivo, although it should also be noted that the variants are not located in the predicted binding pocket for citalopram (26, 27). We also found equivalent citalopram recognition by GK/ER variants in our transfection studies (Fig. S4).

A larger physiological significance of mSERT GK/ER variation becomes most evident via inspection of archived phenotypes associated with lines segregating the ER/GK haplotype. An important strength of this approach is that traits assessed in this paradigm do not derive from a priori functional hypotheses, although by necessity they reflect the interests of the research community using RI lines. In this effort, we found a significant impact of the GK haplotype on body weight, confirmed by our own assessments (data not shown) and the known anorexigenic action of elevated extracellular 5-HT (28, 29). We were struck by the multiple associations between the GK haplotype and ethanol-related behaviors, where the GK low-uptake activity is associated with lower ethanol consumption and acceptance. In humans, individuals with the low-functioning S allele of the 5HTTLPR, and presumably increased synaptic 5-HT availability, demonstrate lower voluntary ethanol consumption (30, 31). These findings also point to further utility of gene × environment designs in analysis of the functional impact of the ER/GK haplotype.

Possibly, the associations of the ER/GK haplotype with ethanol sensitivity/consumption traits relate to a more global modulation of reward pathways, such as those through which DA signaling modulates reinforcement. Consistent with this idea, we found the ER/GK haplotypes to associate with altered DAT and D2 receptor expression. DAT and D2 receptor expression are known to be under significant genetic influence (29, 32). Importantly, serotonergic innervation regulates both somatic DA neuron excitability and terminal field DA release (33, 34).

Although it is reasonable to expect that ER/GK haplotype-driven differences in SERT activity impact DA signaling directly, we identified an indirect pathway involving midbrain iron homeostasis that may have even larger significance. A 3-way association between SERT, iron, and dopaminergic traits cannot alone define epistatic relationships. However, our evaluation of SERT knockout mice, where we observed a significant reduction in midbrain iron levels in SERT KO mice relative to controls, raises the possibility that 5-HT signaling has a significant effect on dopaminergic traits via the control of mesencephalic and basal ganglia iron homeostasis. The rate-limiting step in the production of dopamine is the activity of tyrosine hydroxylase, an iron-requiring enzyme (35, 36). Additionally, 5-HT, acting via 5-HT2C receptors in the choroid plexus, regulates transferrin receptor expression (37). Region-specific alterations in iron homeostasis in SERT KO mice indicate additional factors key to iron sequestration that may also be differentially impacted by 5-HT signaling. Importantly, dietary iron reductions produce reversible reductions in CNS DAT and D2 receptor expression (38, 39).

An important, additional strength of studies examining natural gene variation in murine RI strains, is the opportunity to characterize the impact of genetic interactions in defining complex traits. For example, BXD lines also exhibit functional variation at the locus encoding the enzyme responsible for CNS 5-HT synthesis, *Tph2* (18). C57BL/6J inbred mice express the high-functioning *Tph2* allele and, as we have shown, a low-functioning SERT variant. Synaptically, this would suggest that in C57BL/6J, high levels of 5-HT production and release are accompanied by relatively low rates of 5-HT clearance. In contrast, DBA/2J mice express the low-functioning *Tph2* Arg-447 variant in the context of a high-functioning mSERT ER variant. Here, the predicted effect is relatively reduced 5-HT synthesis and release in the context of high 5-HT clearance capacity. Together, these allelic combinations are predicted to drive ceiling and floor levels of synaptic 5-HT in B and D RI lines, respectively. The designation of mSERT and *Tph2* variants in these lines is but one example of an advancing sophistication in our understanding of how to model 5-HT impact on complex traits, many of which are routinely used to model components of neuropsychiatric disease risk and the effects of medications (40, 41).

Experimental Procedures

Cell Transfections and Transport Assays. The Stratagene QuikChange kit was used to generate the coding mutants in the mSERT/pcDNA3.1. Mutants were confirmed by fluorescent DNA sequencing (Center for Molecular Neuroscience, Neurogenomics and Sequencing Core Facility, Vanderbilt University Nashville, Tennessee). HeLa cells were transfected and [^{3}H] 5-HT uptake was performed as previously described (42). K_M and V_{MAX} values obtained from evaluation of transport activity were derived using a nonlinear curve fit as a function of 5-HT concentration (100 nM to 10 μM) (Prism4 for PC, Graphpad software). We normalized total uptake data by the mSERT expression levels obtained by Western blot analysis of each individual experiment. All experiments were performed in triplicate and repeated in 6 or more separate assays.

Synaptosomal Uptake and Binding. Mouse studies were performed in accordance with humane guidelines established by the Vanderbilt Institutional Animal Care and Use Committee (IACUC) under an approved protocol (M/04/376). Inbred mice were obtained from The Jackson Laboratory (Bar Harbor, Maine) and killed at 8–10 weeks of age. BXD male mice were obtained from the University of Tennessee Health Science Center and Oak Ridge National Laboratory. Brain tissue was dissected and homogenized for synaptosomal uptake and binding as described previously (43). The following BXD lines were used: ER lines: 44, 61, 60, 77, 90, and 97 (n = 26) and GK lines: 83, 75, 40, 66, 31, 76, and 56 (n = 24).

Tail Suspension Test. Basal TST was performed manually by 2 independent researchers blind to genotype. Each mouse was suspended by its tail and total

duration of immobility was calculated as the time the mouse became immobile during a 6-min test session. Mice that either climbed the apparatus or failed to exhibit immobility were removed from the analysis. For analysis of basal TST, unpaired Student's *t tests* were used to compare in 7 GK BXD lines (nos. 31, 40, 56, 66, 75, 76, and 83; $n = 23$) and 7 ER BXD lines (nos. 44, 60, 61, 77, 90, 96, and 97; $n = 26$). For the SSRI sensitivity studies, we used the BXD lines: nos. 89 ,61, 69, 51, 90, 48, 67, 97, 43, 92 (ER, $n = 88$) and 66, 75, 50, 11, 9, 40, 31, 45, 39, 63 (GK, $n = 71$). Racemic citalopram hydrobromide was prepared fresh daily by dissolving the powder in deionized water. Drug was administered by i.p. injection in a volume of 0.01 mL/g body weight and the dose was 20 mg/kg calculated as the weight of the base. Control animals received injections of 0.9% saline in a volume of 0.01 mL/g. Each mouse was tested twice in the TST: once with saline and once with citalopram, 1 week apart. A counterbalanced design was used, where half of the animals received saline followed by citalopram and the other half received citalopram followed by saline. Mice were injected with drug or saline 30 min before a 6-min tail suspension test. An automated TST device (Med Associates, St. Albans, Vermont) was used to measure the duration of behavioral immobility. Mice were suspended by the tail with tape to a vertical aluminum bar connected to a strain gauge. The following settings were used in all experiments: threshold 1, 7; gain, 8; time constant, 0.25; and resolution, 200 ms.

Open Field Activity Test. Exploratory locomotor activity was evaluated using commercially available 27.9 × 27.9 cm activity monitors (MED Associates, Georgia, Vermont) in standard fluorescent light. Mice were placed in the monitors 90 min and allowed to explore freely. Data were exported in 10-min time bins over 90 min and 1-min time bins during the first 10 min. For analysis, unpaired Student's *t tests* were used, comparing the cumulative data obtained in the first 10 min of activity. BXD lines with the GK haplotype were nos. 11, 31, 39, 40, 45, 50, 63, 66, and 75 ($n = 53$). BXD lines with the ER haplotype were nos. 43, 48, 51, 61, 67, 69, 73, 89, 90, 92, 97 ($n = 86$).

In Silico Analysis of BXD Phenotypes. Eight hundred forty-three BXD recombinant inbred phenotypes were downloaded from Genenetwork.org (August 2007) and tested for association with the functional GK/ER *Slc6a4* haplotype and the Arg447Pro *Tph2* SNP. The genotype for the gene *Tph2* was inferred from the marker rs4228477. Both an epistatic linear model (ANOVA) and an additive linear model for genotypes at rs13481111 and rs4228477 were examined for phenotypes with 12 or more strains measured (average 24 strains total, average 6 per genotype combination). We set the cutoff for interest at an alpha of 0.05 for model omnibus tests, because of the exploratory nature of this aspect of the study (data shown in Fig. S3 and Tables S2 and S3). The phenotypes that were significantly altered by mSERT haplotype were then tested in unpaired *t tests*, as shown in Fig. S3.

Brain Region Iron Analysis. Tissue iron concentrations were measured with graphite furnace atomic absorption spectroscopy (Varian AA240, Varian). Brain regions were digested in ultrapure nitric acid (1:10 wt/vol dilution) for 48–72 h in a sand bath (60°C). An aliquot of 50 μL of digested tissue was brought to 1 mL of total volume with 2% nitric acid and analyzed for Fe. Bovine liver (National Bureau of Standards, U.S. Department of Commerce, Washington, DC) (10 μg of Mn/g; 184 μg of Fe/g) was digested in ultrapure nitric acid and used as an internal standard for analysis (final concentration 92 μg of Fe/L) to ensure consistency between runs.

ACKNOWLEDGMENTS. We are grateful to Rob Williams (University of Tennessee Health Science Center) for provision of RI lines. We thank Michael Aschner for helpful discussion during the development of the project. We gratefully acknowledge Jane Wright for animal husbandry and support in the behavior tasks and Qiao Han for tissue culture support. We also thank Ray Johnson and Denise Malone from the Center for Molecular Neuroscience Neurochemistry and Neurogenomics cores, for neurochemistry and DNA sequencing support. We acknowledge support from MH65215, MH65782 (A.M.D.C.), 2005 NARSAD Young Investigator Award (C.B.Z.), U01AA014425 (L.L.), NINDS 1R15NS061309–01 (K.M.E.), and DA07390 and MH07828 (R.D.B.). D.C.A. acknowledges support from Alfred L. George Jr. and the Vanderbilt Institute for Integrative Genomics. B.T. was supported by Institutional Research and Academic Career Development Award GM068543 to R.C. and by National Institutes of Health Award DA00390 (to R.D.B.). E.C. acknowledges funding from National Institute on Alcohol Abuse and Alcoholism (U01AA13499 and U24AA13513), National Institute on Drug Abuse R01DA020677, and Department of Energy Office of Biological and Environmental Research under contract DE-AC05–00OR22725 with University of Tennessee-Battelle, LLC.

1. Azmitia EC (2007) Serotonin and brain: evolution, neuroplasticity, and homeostasis. *Int Rev Neurobiol* 77:31–56.
2. Blakely RD, *et al.* (1991) Cloning and expression of a functional serotonin transporter from rat brain. *Nature* 354:66–70.
3. Torres GE, Gainetdinov RR, Caron MG (2003) Plasma membrane monoamine transporters: structure, regulation and function. *Nat Rev Neurosci* 4:13–25.
4. Bengel D, *et al.* (1998) Altered brain serotonin homeostasis and locomotor insensitivity to 3, 4-methylenedioxymethamphetamine (''Ecstasy'') in serotonin transporter-deficient mice. *Mol Pharmacol* 53:649–655.
5. Thakker DR, *et al.* (2005) siRNA-mediated knockdown of the serotonin transporter in the adult mouse brain. *Mol Psychiatry* 10:782–789,714.
6. Zhao S, *et al.* (2006) Insertion mutation at the C-terminus of the serotonin transporter disrupts brain serotonin function and emotion-related behaviors in mice. *Neuroscience* 140:321–334.
7. Jennings KA, *et al.* (2006) Increased expression of the 5-HT transporter confers a low-anxiety phenotype linked to decreased 5-HT transmission. *J Neurosci* 26:8955–8964.
8. Murphy DL, Lesch KP (2008) Targeting the murine serotonin transporter: insights into human neurobiology. *Nat Rev Neurosci* 9:85–96.
9. Chesler EJ, *et al.* (2005) Complex trait analysis of gene expression uncovers polygenic and pleiotropic networks that modulate nervous system function. *Nat Genet* 37:233–242.
10. Holmes A, Lit Q, Murphy DL, Gold E, Crawley JN (2003) Abnormal anxiety-related behavior in serotonin transporter null mutant mice: the influence of genetic background. *Genes Brain Behav* 2:365–380.
11. Peirce JL, Lu L, Gu J, Silver LM, Williams RW (2004) A new set of BXD recombinant inbred lines from advanced intercross populations in mice. *BMC Genet* 5:7.
12. Williams RW, Gu J, Qi S, Lu L (2001) The genetic structure of recombinant inbred mice: high-resolution consensus maps for complex trait analysis. *Genome Biol* 2:RESEARCH0046.
13. Tsaih SW, Lu L, Airey DC, Williams RW, Churchill GA (2005) Quantitative trait mapping in a diallel cross of recombinant inbred lines. *Mamm Genome* 16:344–355.
14. Gatti D, *et al.* (2007) Genome-level analysis of genetic regulation of liver gene expression networks. *Hepatology* 46:548–557.
15. Dong H, *et al.* (2007) Quantitative trait loci linked to thalamus and cortex gray matter volumes in BXD recombinant inbred mice. *Heredity* 99:62–69.
16. Chesler EJ, *et al.* (2008) The Collaborative Cross at Oak Ridge National Laboratory: developing a powerful resource for systems genetics. *Mamm Genome* 19:382–389.
17. Churchill GA, *et al.* (2004) The Collaborative Cross, a community resource for the genetic analysis of complex traits. *Nat Genet* 36:1133–1137.
18. Zhang X, Beaulieu JM, Sotnikova TD, Gainetdinov RR, Caron MG (2004) Tryptophan hydroxylase-2 controls brain serotonin synthesis. *Science* 305:217.
19. Holmes A, Yang RJ, Lesch KP, Crawley JN, Murphy DL (2003) Mice lacking the serotonin transporter exhibit 5-HT(1A) receptor-mediated abnormalities in tests for anxiety-like behavior. *Neuropsychopharmacology* 28:2077–2088.
20. Lira A, *et al.* (2003) Altered depression-related behaviors and functional changes in the dorsal raphe nucleus of serotonin transporter-deficient mice. *Biol Psychiatry* 54:960–971.
21. Li X, Morrow D, Witkin JM (2006) Decreases in nestlet shredding of mice by serotonin uptake inhibitors: comparison with marble burying. *Life Sci* 78:1933–1939.
22. Jones MD, Lucki I (2005) Sex differences in the regulation of serotonergic transmission and behavior in 5-HT receptor knockout mice. *Neuropsychopharmacology* 30:1039–1047.
23. Boyce-Rustay JM, *et al.* (2006) Ethanol-related behaviors in serotonin transporter knockout mice. *Alcohol Clin Exp Res* 30:1957–1965.
24. Daws LC, *et al.* (2006) Ethanol inhibits clearance of brain serotonin by a serotonin transporter-independent mechanism. *J Neurosci* 26:6431–6438.
25. Jones BC, *et al.* (2003) Quantitative genetic analysis of ventral midbrain and liver iron in BXD recombinant inbred mice. *Nutr Neurosci* 6:369–377.
26. Barker EL, Blakely RD (1998) Structural determinants of neurotransmitter transport using cross-species chimeras: studies on serotonin transporter. *Methods Enzymol* 296:475–498.
27. Henry LK, *et al.* (2006) Tyr-95 and Ile-172 in transmembrane segments 1 and 3 of human serotonin transporters interact to establish high affinity recognition of antidepressants. *J Biol Chem* 281:2012–2023.
28. Garattini S, Bizzi A, Codegoni AM, Caccia S, Mennini T (1992) Progress report on the anorexia induced by drugs believed to mimic some of the effects of serotonin on the central nervous system. *Am J Clin Nutr* 55:160S–166S.
29. Buck K, Lischka T, Dorow J, Crabbe J (2000) Mapping quantitative trait loci that regulate sensitivity and tolerance to quinpirole, a dopamine mimetic selective for D(2)/D(3) receptors. *Am J Med Genet* 96:696–705.
30. Hallikainen T, *et al.* (1999) Association between low activity serotonin transporter promoter genotype and early onset alcoholism with habitual impulsive violent behavior. *Mol Psychiatry* 4:385–388.
31. Kranzler H, Lappalainen J, Nellissery M, Gelernter J (2002) Association study of alcoholism subtypes with a functional promoter polymorphism in the serotonin transporter protein gene. *Alcohol Clin Exp Res* 26:1330–1335.
32. Janowsky A, *et al.* (2001) Mapping genes that regulate density of dopamine transporters and correlated behaviors in recombinant inbred mice. *J Pharmacol Exp Ther* 298:634–643.
33. Herve D, Pickel VM, Joh TH, Beaudet A (1987) Serotonin axon terminals in the ventral tegmental area of the rat: fine structure and synaptic input to dopaminergic neurons. *Brain Res* 435:71–83.

34. Lieberman JA, *et al.* (1998) Serotonergic basis of antipsychotic drug effects in schizophrenia. *Biol Psychiatry* 44:1099–1117.
35. Nagatsu T (1995) Tyrosine hydroxylase: human isoforms, structure and regulation in physiology and pathology. *Essays Biochem* 30:15–35.
36. Bianco LE, Wiesinger J, Earley CJ, Jones BC, Beard JL (2008) Iron deficiency alters dopamine uptake and response to L-DOPA injection in Sprague–Dawley rats. *J Neurochem* 106:205–215.
37. Esterle TM, Sanders-Bush E (1992) Serotonin agonists increase transferrin levels via activation of 5-HT1C receptors in choroid plexus epithelium. *J Neurosci* 12:4775–4782.
38. Beard JL, Chen Q, Connor J, Jones BC (1994) Altered monamine metabolism in caudate-putamen of iron-deficient rats. *Pharmacol Biochem Behav* 48:621–624.
39. Connor JR, *et al.* (2008) Comparative study of the influence of Thy1 deficiency and dietary iron deficiency on dopaminergic profiles in the mouse striatum. *J Neurosci Res* 86:3194–3202.
40. Sanders-Bush E, Fentress H, Hazelwood L (2003) Serotonin 5-ht2 receptors: molecular and genomic diversity. *Mol Interv* 3:319–330.
41. Serretti A, Benedetti F, Zanardi R, Smeraldi E (2005) The influence of serotonin transporter promoter polymorphism (SERTPR) and other polymorphisms of the serotonin pathway on the efficacy of antidepressant treatments. *Prog Neuropsychopharmacol Biol Psychiatry* 29:1074–1084.
42. Zhu CB, Hewlett WA, Feoktistov I, Biaggioni I, Blakely RD (2004) Adenosine receptor, protein kinase G, and p38 mitogen-activated protein kinase-dependent up-regulation of serotonin transporters involves both transporter trafficking and activation. *Mol Pharmacol* 65:1462–1474.
43. Ramamoorthy S, Samuvel DJ, Buck ER, Rudnick G, Jayanthi LD (2007) Phosphorylation of threonine residue 276 is required for acute regulation of serotonin transporter by cyclic GMP. *J Biol Chem* 282:11639–11647.